CONTROL OF SOLID–STATE TRANSFORMERS FOR WIND POWER INTERFACING

A PROJECT REPORT

Submitted by

KEERTHI GOPAL D

TKM20EEPS08

to

the **APJ Abdul Kalam Technological University**

in partial fulfillment of the requirements for the award of the Degree

of

Master of Technology

In

Power Systems

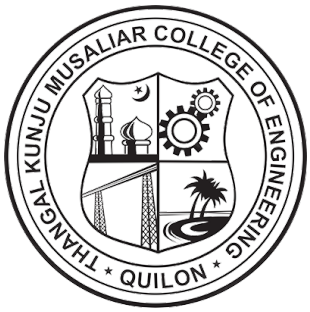

DEPARTMENT OF ELECTRICAL & ELECTRONICS ENGINEERING

T.K.M COLLEGE OF ENGINEERING

KOLLAM-5

2020-2022

DEPARTMENT OF ELECTRICAL & ELECTRONICS ENGINEERING

THANGAL KUNJU MUSALIAR COLLEGE OF ENGINEERING

KOLLAM

CERTIFICATE

This is to certify that the project report titled **'CONTROL OF SOLID–STATE TRANSFORMERS FOR WIND POWER INTERFACING'** submitted by **Ms. KEERTHI GOPAL D**., to the APJ Abdul Kalam Technological University in partial fulfillment of the requirements for the award of the Degree of Master of Technology in Power Systems, Electrical & Electronics Engineering is a bonafide record of the project work carried out by her under our guidance and supervision. This report in any form has not been submitted to any other University or Institute for any purpose.

Prof. SHANAVAS T N
Associate Professor
[Internal Supervisor & PG Coordinator]
Department of Electrical and Electronics

(EXTERNAL EXAMINER)

Dr. SABEENA BEEVI K
Associate Professor [HOD]
Department of Electrical and Electronics

ACKNOWLEDGEMENT

I am obediently thankful to **God Almighty**, praise and glory is to Him, for all His uncountable bounties and guidance, without which, this project would have never been a reality.

It is my privilege and pleasure to express my gratitude and indebtedness to **Dr. T A Shahul Hameed**, Principal of TKM College of Engineering, and **Dr. Sabeena Beevi K**, Associate Professor, Head of the Department, Electrical and Electronics Dept, for providing all the required resources for the completion of my project work.

My heartfelt gratitude to **Prof. Shanavas T N**, Associate Professor, PG Coordinator and Internal Supervisor, Electrical and Electronics Dept, and **Mr. Naufal N**, for his valuable suggestions and guidance in designing and implementing this project.

I express my thanks to **Prof. Jibi P Mathew**, Asst. Professor, Project Coordinator, Electrical and Electronics Dept, for all help and coordination in completing this project successfully and on time.

I will be failing in duty if I do not acknowledge the authors of the references and other pieces of literature referred to in this project.

I show my extreme gratitude to all Faculty member and Technical staffs in Electrical and Electronics Dept, for providing all the help and necessary facilities to complete the project work and my deep hearted cheers to my parents and all my friends who extended their support and co-operation towards the successful completion of the project.

KEERTHI GOPAL D

ABSTRACT

Use of renewable energy sources (RES) due to population growth and decentralization is increasing all over the world. Urbanization and consideration for the environment also contribute to the increased use of RES. With advancements in turbine and battery storage technology, the use of wind power has increased significantly. Of the total amount of installed renewable energy capacity of India, 68% of the total production is from wind energy. The intermittent nature of wind energy and related power quality issues like voltage flashing and harmonics, however, provide a substantial barrier. By integrating wind energy into the grid utilising solid state transformers (SST), this issue can be resolved. The regulated and unregulated DC link voltages on either side of the SST are coupled by the DC-DC converter component of the SST. To obtain regulated output voltage, the current-fed PWM PS (Phase Shifted) controlled full bridge converter is controlled. A Single Active Bridge (SAB) based SST is utilised for wind energy integration to prevent the circuit's complexity and to give ease of control. The performance of the system is studied for varying wind speeds using PI, PID and Fuzzy-PID controllers and their performances are compared. The system performance after introduction of a disturbance is also studied. The system is simulated using SIMULINK in MATLAB software.

Contents

ACKNOWLEDGEMENT **i**

ABSTRACT **ii**

LIST OF FIGURES **v**

LIST OF TABLES **vii**

ABBREVIATIONS **viii**

1 INTRODUCTION **1**

1.1 General Background 1

1.2 Motivation 3

1.3 Thesis objectives 4

1.4 Structure of thesis 4

1.4.1 Chapter 1 4

1.4.2 Chapter 2 5

1.4.3 Chapter 3 5

1.4.4 Chapter 4 5

1.4.5 Chapter 5 5

2 LITERATURE REVIEW **6**

2.1 Introduction 6

2.2 Related Works 6

3 SYSTEM MODELING **9**

3.1 Introduction 9

3.2 System Architecture 9

3.2.1 SAB Converter 11

3.3 System Modeling 12

3.3.1 Wind Turbine 12

3.3.2 Two Mass Drive Train 13

3.3.3 Permanent Magnet Synchronous Generator 14

4 METHODOLOGY **15**

4.1 Introduction 15

4.2 PI Controller 15

4.3 PID Controller 16

4.4 Fuzzy-PID Controller 17

5 RESULTS AND DISCUSSION **23**

5.1 Introduction 23

5.2 Results- Closed loop system 25

5.2.1 Closed loop simulation- PI Controller 25

5.2.2 Closed loop simulation- PID Controller 25

5.2.3 Closed loop simulation- Fuzzy-PID Controller 28

5.2.4 Analysis 28

5.3 Results- Disturbance analysis 30

6 CONCLUSION **34**

PUBLICATIONS **35**

REFERENCES **36**

List of Figures

1.1 Medium and low voltage distribution systems with a) conventional transformer, b) solid state transformer[5]. 2

3.1 Various SST topology configurations (a) Single-stage topology; (b) Two-stage topology with low voltage DC link; (c) Two-stage topology with high voltage DC link; (d)Three-stage topology [**?**]. 9

3.2 Application of SST in integrating wind power conversion system. 10

3.3 Block diagram of Single Active Bridge(SAB) converter. 11

3.4 Simulink diagram of wind turbine model. 12

3.5 Simulink diagram of pitch angle controller. 13

3.6 Simulink diagram of two mass drive train. 14

4.1 Block diagram of dual PI-tuned controller for SAB converter. 16

4.2 Block diagram of dual PID-tuned controller for SAB converter. 16

4.3 Schematic diagram of Fuzzy controller. 17

4.4 Representation of triangular membership function. 18

4.5 Membership funtions of inputs: (a) Error (b) Change in error 20

4.6 Membership funtions of outputs: (a) K_P (b) K_I (c) K_D 21

4.7 Block diagram of Fuzzy-PID controller for SAB converter. 22

5.1 Block diagram of proposed system in MATLAB/SIMULINK. 24

5.2 Block diagram of WECS in MATLAB/SIMULINK. 24

5.3 Simulation of system with dual PI-tuned controller. 26
5.4 Voltage across HVDC link capacitor with dual PI-tuned controller. 26
5.5 Simulation of system with dual PID-tuned controller. 27
5.6 Voltage across HVDC link capacitor with dual PID-tuned controller. 27
5.7 Simuation of system with Fuzzy-PID controller. 28
5.8 Simulink diagram of Fuzzy-PID controller. 29
5.9 Voltage across HVDC link capacitor with Fuzzy-PID controller. 29
5.10 Simulation of system having dual PI-tuned controller with disturbance introduced at 0.8s. 31
5.11 Voltage across HVDC link capacitor with dual PI-tuned controller with disturbance. 31
5.12 Simulation of system having dual PID-tuned controller with disturbance introduced at 0.8s. 32
5.13 Voltage across HVDC link capacitor with dual PID-tuned controller with disturbance. 32
5.14 Simulation of system having Fuzzy-PID controller with disturbance introduced at 0.8s. 33
5.15 Voltage across HVDC link capacitor with Fuzzy-PID controller with disturbance. 33

List of Tables

5.1 Simulation Parameters 25
5.2 Comparison of controller performances 30

ABBREVIATIONS

COA	Centre of Area
DAB	Dual Active Bridge
DDSG	Directly Driven Synchronous Generator
DER	Distributed Energy Resources
DFIG	Doubly-fed Induction Generator
FLC	Fuzzy Logic Controller
HFT	High Frequency Transformer
LFT	Low Frequency Transformer
LV	Low Voltage
MATLAB	Matrix Laboratory
MV	Medium Voltage
PMSG	Permanent Magnet Synchronous Generator
PS	Phase Shifted
PWM	Pulse Width Modulated
RES	Renewable Energy Sources

SAB	Single Active Bridge
SST	Solid State Transformer
ST	Smart Transformer
WECS	Wind Energy Conversion System

Chapter 1

INTRODUCTION

1.1 General Background

Globally, the usage of distributed energy resources (DER) and other renewable energy sources (RES) has grown in tandem with population growth and decentralisation. Urbanization and concern for environment has also driven the rise in the use of RES. However, the uneven nature of various RES such as solar and wind power and the associated power quality issues such as voltage flashing, harmonics and need for reactive power compensation poses a major obstacle. To address these issues, new technologies are necessary for improved control and more reliable grid operation. In wind power conversion systems, a transformer which steps up voltage at fundamental frequency acts as the link between the turbine and the grid. Recent attempts to switch from the traditional transformer to a more sophisticated solid state transformer have been made in an effort to address these difficulties.

A Solid–State Transformer (SST) also known as Smart Transformer (ST) is a transformer that operates at high frequency that is composed of power electronic converters which takes the place of conventional transformer. It offers all the functionalities of a

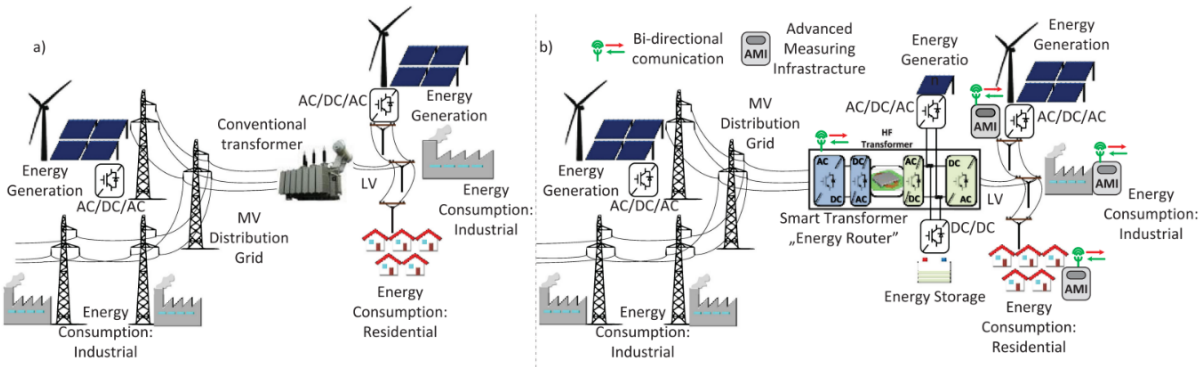

Figure 1.1. Medium and low voltage distribution systems with a) conventional transformer, b) solid state transformer[5].

classical transformer, in addition to various auxiliary services for the connection of DC and AC equipments. Additionally, it enables surge protection, bidirectional power flow, reactive power compensation, voltage regulation, and a reduction in voltage drops as well as short-circuit currents, harmonics, and DC connections. The major feature of an ST is its ability to integrate RES, electric vehicles and energy storage systems into the grid. By using a smart transformer instead of a conventional transformer, there is compensation of nonlinear currents of low voltage loads in grid, thereby improving the power quality by the reduction of harmonics in current. In spite of reactive power and unbalanced loads connected to the LV grid, the SST has the ability to maintain current that is symmetrical with unity power factor. Hence the transmitted energy is only dependent upon the active power, thus reducing the losses during transmission. Various control strategies for ST can be applied depending upon the application. Also, there is improvement in voltage at the node where the SST is connected, which impacts the other nodes in the grid. However, depending on the line impedances and the rated power of the ST, the procedure can be limited or need power oversizing of the ST. The weight and size reduction of SST over a typical distribution transformer is an noticeable advantage. A comparison study of the conventional with the solid state transformer shows that the size of the SST is 80% less than that of an LFT. Fig.1.1 shows medium and low voltage distribution systems with

conventional and solid state transformer.

Generally, in wind energy conversion systems (WECS), two types of generators—the doubly fed induction generator (DFIG) and the permanent magnet synchronous generator (PMSG)—are employed for conversion purposes. The disadvantage of DFIG is that it needs a gear box to match the rotor and turbine speeds. PMSG has the a number of advantages over DFIG like better reliability, higher efficiency, reduced losses and better controllability. A PMSG without a gearbox requires more number of poles and vice-versa. A PMSG based WECS is used to generate low voltage input in this paper. Variable speed operation is achieved by varying the wind speed from 20 to 25m/s. The performance of the system is studied for varying wind speeds using PI, PID and Fuzzy-PID controllers and their performances are compared. The system performance after introduction of a disturbance is also studied. The system is simulated using SIMULINK in MATLAB software.

1.2 Motivation

Around the world, almost 2.5 lakhs MW energy is produced every year. 10% of this energy is stored and 16% is annual demand of consumers. The remaining need is met with other sources of energy. About 60% of energy is produced using non-renewable sources like coal and fossil fuels. About 12% of energy is produced using RES such as solar and wind. About 40% of this is contributed by WECS and 4% is produced from solar energy conversion systems. WECS has more efficiency and is implemented more. The intermittent nature of this source however causes various power quality and stability issues and calls for an effective means for their integration into the grid. Solid state transformers can be used for this purpose. The efficiency of these transformers can be greatly improved using suitable controllers like PI, PID and Fuzzy-PID controllers.

1.3 Thesis objectives

The following study areas are defined based on the thorough literature assessment on the subject, and work is done on some of the key problems that is concerned with the integration of WECS into the grid. The major objectives are

- Simulation of PMSG based WECS.
- Simulation of closed loop system with PI Controller.
- Simulation of closed loop system with PID Controller.
- Simulation of closed loop system with Fuzzy-PID Controller.
- Study and compare the performance of system with PI, PID and Fuzzy-PID Controllers.
- Study and compare the performance of system with PI, PID and Fuzzy-PID Controllers after the introduction of disturbance.
- Achieve improved voltage regulation, reduced steady state error, rise time, settling time and peak overshoot of output voltage of SAB (Single Active Bridge) DC-DC converter.

1.4 Structure of thesis

1.4.1 Chapter 1

This chapter's introduction emphasises the advantages of using renewable energy sources like wind energy over traditional energy sources. The use of solid state transformer is discussed in the chapter as a means of overcoming the difficulties associated with incorporating wind energy sources into the grid. A comparison of SST is made against conventional

transformers and PMSG is made against DFIG. This also briefly describes the thesis's inspiration, goal, and structure.

1.4.2 Chapter 2

This chapter addresses the literature reviewed for the implementation of the project. Various existing literature on fields related to the proposed system were comprehensively studied and analysed.

1.4.3 Chapter 3

This chapter addresses the modeling of the system. Analysis is done on the system's entire architecture. It contains a mathematical model of the various WECS components, that is the wind turbine, two mass drive train and PMSG. The simulation diagrams for the various WECS components are also included.

1.4.4 Chapter 4

Chapter 4 focuses on the brief introduction of PI, PID and Fuzzy-PID controllers. The implementation of the various controllers in the system is extensively explained.

1.4.5 Chapter 5

The simulations, findings, and comments are covered in this chapter. System is simulated in SIMULINK under MATLAB software. System performance is also observed after the introduction of a disturbance. Results of different controllers are compared and analysed.

Chapter 2

LITERATURE REVIEW

2.1 Introduction

The literature that was reviewed for the project's execution is covered in this chapter. It describes distributed generation sources, its benefits and drawbacks in detail. A number of power quality challenges arise when they are connected to the grid. On comparison of conventional transformer against solid state transformer, the latter offers a number of advantages. And hence, they are a better option for integration of WECS into the grid.

2.2 Related Works

[1] E.J. Coster, J.M.A Myrzik, B. Kruimer, and W. L. Kling(2011), "Integration Issues of Distributed Generation in Distribution Grids,"Proceedings of the IEEE, vol. 99, no. 1. The paper discusses the distributed generation sources in detail. Distributed generation is the localized, small scale generation of electricity. It offers a number of benefits like flexibility in price response, reliability needs and power quality needs. They offer effective compromise transmission and distribution costs. However, high cost is a disadvantage. It becomes difficult to predict the power and there is less choices for selection of primary fuels.

[2] X. Liang(2017), "Emerging power quality challenges due to integration of renewable energy sources," IEEE Transactions on Industrial Applications, vol. 53. This paper discusses the various power quality issues introduced on integrating RES like wind, solar and geothermal into the grid. Harmonics, voltage and frequency fluctuations are the main power quality issues. Voltage and frequency fluctuations occur due to the uncontrollable and variable nature of RES. Power electronic converters used in the production of renewable energy are to blame for harmonics. As the penetration of renewable sources increases, the level of harmonics becomes more significant.

[3] A. Milczarek and M. Malinowski(2019), "Comparison of classical and smart transformers impact on MV distribution grid," IEEE Transactions on Power Delivery, vol. 30. Compared to CT, SST offers a number of advantages like high efficiency, functionality, reduced size and weight, etc. At the same time, SST has a number of drawbacks like high complexity, reduced overload and short-circuit capability, etc.

[4] Imran Syed, and Vinod Khadkikar(2017), "Replacing the Grid Interface Transformer in Wind Energy Conversion System With Solid-State Transformer,"IEEE Transactions on Power Systems, vol. 32, no. 3.

Here, the conventional transformer is replaced with a smart transformer. The smart transformer couples the DFIG based WECS to the utility grid. Conventional transformers have a number of disadvantages like harmonics, environmental impacts, large size, difficult to transport, etc. These drawbacks can be rectified with the help of a smart transformer.

[5] J. Subhadeep Paladhi and Ashok S(2015), "Power Quality Improvements in Wind Based DG Systems using Solid State Transformer," International Journal of Scien- tific Engineering Research, vol. 6, no. 4.

Wind power is being increasingly integrated into the grid. However, there are a variety of power quality problems, such as reactive power compensation and reduced system stability. This study examines how solid state transformers can be used to improve power factor, reduce voltage sag and swell at the point of common coupling, and other power quality issues. Wind farms based on three types of machines, that is, SCIG, DFIG and

DDSG are compared and it is observed that they consume the most reactive power.

[6] S. Falcones, X. Mao, and R. Ayyanar(2010), "Topology comparison for solid state transformer implementation,"in Proc. IEEE PES Gen. Meeting. There are several topologies for SST, including single-stage, two-stage, and three-stage. Compared to the three stage topology, the other configurations have some drawbacks. They do not support bidirectional power flow and interconnection of RES. To effective replace a conventional transformer, the SST should have atleast one DC link. DAB based three-stage topology is the best option for SST integration into the grid.

Chapter 3

SYSTEM MODELING

3.1 Introduction

The proposed system consists of a PMSG based WECS connected to SST. The WECS is based on PMSG due to its various advantages such as absence of rotor losses, soft starting ability and magnetization property provided by the permanent magnets

3.2 System Architecture

Considering the difference in converter topologies, solid state transformers are generally classified as single-stage trans- formers, two-stage transformers and three-stage transform-

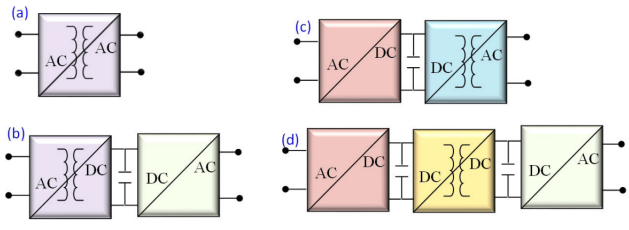

Figure 3.1. Various SST topology configurations (a) Single-stage topology; (b) Two-stage topology with low voltage DC link; (c) Two-stage topology with high voltage DC link; (d)Three-stage topology [**?**].

ers as illustrated in Fig.3.1. Three-stage SST is the most common choice as it optimizes the performance of transmission and distribution grids. It is designed with two DC links to supply and use devices connected to MV or LV and also addresses the various power quality issues. Three stage SST is more superior to other configurations like single stage and two stage in terms of limiting high currents, power factor improvement and regulation of voltage. It is usually used in smart grids which require bidirectional power flow for the flow of power from LV to HV. Hence, three stage topology of SST is considered in this project. A three-stage SST consists of three separate converters: an AC-DC converter in the medium voltage (MV) stage that transforms the three-phase ac voltage at 50 Hz to dc, a DC-DC converter with isolation through a high frequency (HFT) transformer, and finally a DC-AC converter in the low voltage (LV) stage to convert dc voltage to ac at 50Hz. The HFT considerably decreases the overall size of the transformer, making its transportation and installation easier. Proper isolation is necessary to reduce losses and the size of the core. Hence, the core is typically made from nanocrystalline (finemet) or amorphous (vitrovac) based on the type of application. Fig.3.2 depicts the application of SST in wind power integration. The input to the wind energy conversion system (WECS) is wind speed. A 3-phase rectifier is used to convert the 3-phase low voltage input from the wind energy conversion system to DC voltage. A DC-DC converter of the isolated kind with an HFT receives the rectifier's output. The output of second level of ST is fed to a 3-phase inverter which produces a 3-phase output voltage at 50Hz for integration into the

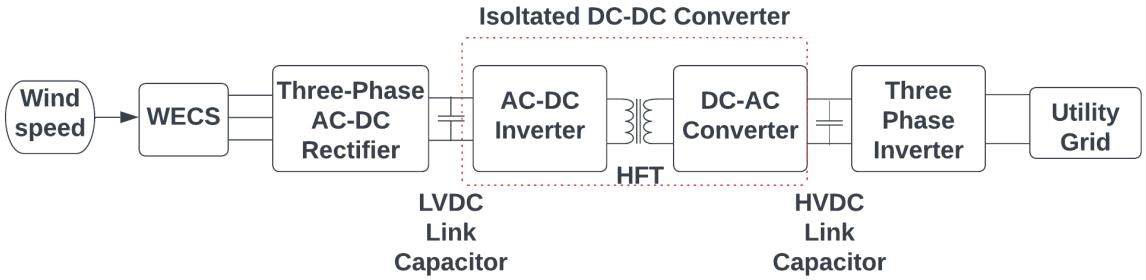

Figure 3.2. Application of SST in integrating wind power conversion system.

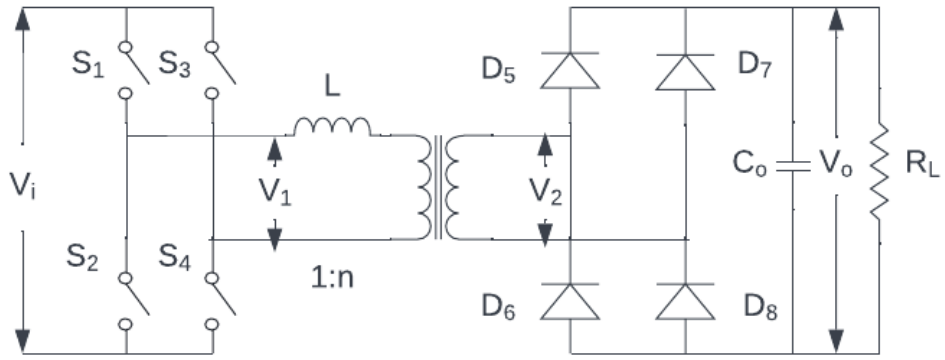

Figure 3.3. Block diagram of Single Active Bridge(SAB) converter.

utility grid.

An isolated type DC-DC converter forms the core of an SST. It links the regulated and unregulated voltages across the DC links on the two sides of the SST. There are various configurations of DC-DC converter that can be implemented. The most popular converters used are the Dual Active Bridge (DAB) converter and Single Active Bridge (SAB) converter. The isolated type DC-DC converter can be controlled to execute the control of the wind power conversion system. For easy analysis and control, an SAB converter is taken for analysis.

3.2.1 SAB Converter

The SAB converter's fundamental block diagram is displayed in Fig.3.3. It has two bridges, separated by an isolating transformer. The input bridge is an active bridge and consists of four switches, S_1 to S_4. The output bridge is a passive bridge and consists of four diodes, D_5 to D_8. The active bridge converts DC to AC and passive bridge converts AC to DC. The isolating transformer has a voltage ratio 1:n and a leakage inductance L. The purpose of the transformer is to provide galvanic isolation. Galvanic isolation is a means to separate the circuits from stray currents that arise due to difference in ground potentials or currents due to AC power. By adjusting the phase of the input bridge legs, the output voltage V_O

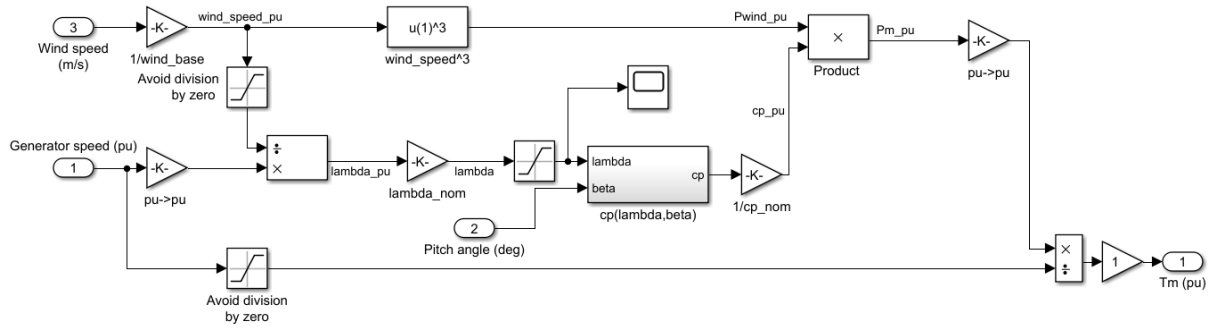

Figure 3.4. Simulink diagram of wind turbine model.

may be adjusted. So there is only one control parameter in this converter, called the phase shift angle.

3.3 System Modeling

Wind turbines are a key component of WECS that transform the kinetic energy of the wind into mechanical energy. The turbine shaft is coupled to the PMSG shaft via a gearbox. The generator's rated torque is produced via the gearbox. Through a solid-state transformer, the generator injects a nominal three-phase voltage into the grid.

3.3.1 Wind Turbine

The wind turbine is responsible for converting the kinetic energy of the wind into the mechanical energy that is then used to produce useful torque. The mechanical energy produced by a wind turbine is given by eqn.3.3.1.

$$P_{\mathrm{m}} = \frac{1}{2}\rho\pi R^2 u^3 C_{\mathrm{p}}(\lambda, \beta) \tag{3.3.1}$$

where ρ is the wind density, π R^2 is the area which is swept by the turbine, u is the speed of wind, θ is the blade angle and $\mathrm{C_p}$ is the power coefficient. The value of $\mathrm{C_p}$ depends upon the characteristics of the turbine, that is the tip speed ratio (λ) and blade pitch angle (β). Fig.3.4 shows the simulink diagram of wind turbine model.

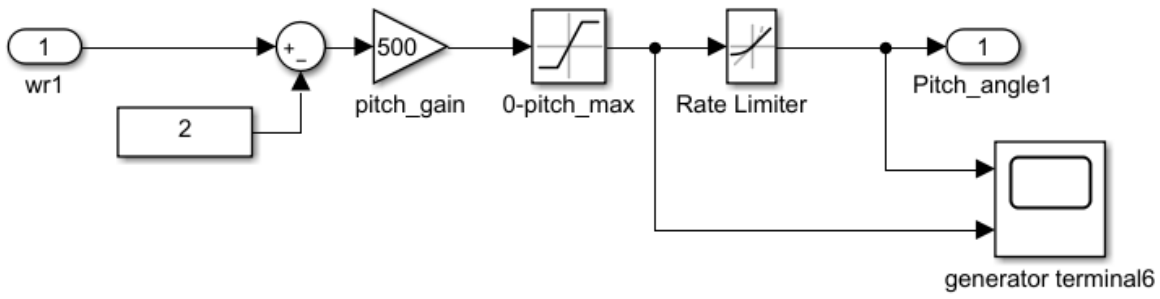

Figure 3.5. Simulink diagram of pitch angle controller.

Tip speed ratio is given as,

$$\lambda = \frac{\Omega_{\mathrm{t}} R}{u} \tag{3.3.2}$$

where Ω_{t} is the speed of the rotor, R is the turbine's radius and u is the speed of wind. C_{p} is obtained by the equation

$$C_{\mathrm{p}}(\lambda, \beta) = c_1 \left[\frac{c_2}{\lambda i} - c_3\beta - c_4\right] exp\left[\frac{-c_5}{\lambda_{\mathrm{i}}}\right] + c_6\lambda \tag{3.3.3}$$

where c_1 to c_6 are various constants which depend on various parameters like rotor blade arrangement, rotor settings and turbine settings.

$$\frac{1}{\lambda_{\mathrm{i}}} = \frac{1}{\lambda + 0.08\beta} - \frac{0.035}{\beta^2} \tag{3.3.4}$$

The pitch angle controller consists of a PI controller. When β becomes zero, λ becomes 6.325 and C_{p} attains the maximum value. Fig.3.5 shows the diagram in simulink for the pitch angle controller.

Then the torque produced by the turbine is calculated as

$$T_{\mathrm{m}} = \frac{P_{\mathrm{m}}}{\Omega_{\mathrm{t}}} \tag{3.3.5}$$

3.3.2 Two Mass Drive Train

Rotor components rotate at a high rpm, whereas wind turbine components rotate at a low rpm. The gearbox raises the wind turbine's low speed to the necessary rotor speed. Fig.3.6

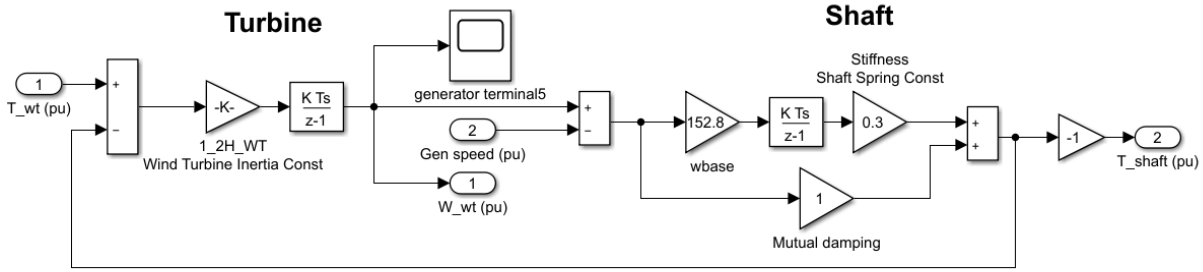

Figure 3.6. Simulink diagram of two mass drive train.

shows the diagram in simulink for a two mass drive train. The mathematical model for a two mass drive train is formulated using eqn.3.3.6 to eqn.3.3.8.

$$2H_{\mathrm{t}}\frac{d\omega_{\mathrm{t}}}{dt} = T_{\mathrm{m}} - T_{\mathrm{s}} \tag{3.3.6}$$

$$\frac{1}{\omega_{\mathrm{ebs}}}\frac{d\theta_{\mathrm{sta}}}{dt} = \omega_{\mathrm{t}} - \omega_{\mathrm{r}} \tag{3.3.7}$$

$$T_{\mathrm{s}} = K_{\mathrm{ss}}\theta_{\mathrm{sta}} + D_{\mathrm{t}}\frac{d\theta_{\mathrm{sta}}}{dt} \tag{3.3.8}$$

Where,

$\mathrm{H_t}$ is the turbines[s] inertia constant, θ_{sta} is the shaft twist angle, ω_{t} and ω_{r} are the angular speed of wind turbine and generator respectively, ω_{ebs} is the electrical base speed, $\mathrm{T_m}$ and $\mathrm{T_s}$ are the mechanical and shaft torques respectively, $\mathrm{K_{ss}}$ is the shaft stiffness and $\mathrm{D_t}$ is the turbine's damping coefficient.

3.3.3 Permanent Magnet Synchronous Generator

The turbine[s] mechanical energy is transformed into electrical energy by the PMSG.The expression for the generating mode of operation of the machine is given as

$$V_{\mathrm{t}} = E_{\mathrm{r}} - I_{\mathrm{a}}(R_{\mathrm{a}} + jX_{\mathrm{L}}) \tag{3.3.9}$$

Chapter 4

METHODOLOGY

4.1 Introduction

The current fed Pulse Width Modulated (PWM) Phase Shifted (PS) controlled full bridge converter in the second stage of SST forms is controlled to achieve improved voltage regulation. When the speed of wind changes, the voltage input to the SST also changes. To keep the output voltage across the HVDC link capacitor constant, the SAB converter is run by a PI, PID, and fuzzy PID controller.

4.2 PI Controller

The proportional and integral control actions of the PI controller make it a versatile controller. The control signal exhibits proportionality with the error signal as well as the integral of the error signal. The general transfer function of a PI controller is given as

$$G(s) = K_{\mathrm{P}}[1 + \frac{1}{sT_{\mathrm{I}}}] \tag{4.2.1}$$

Where, $\mathrm{T_i}=\frac{K_{\mathrm{P}}}{K_{\mathrm{I}}}$ is the integral time constant.

Two PI controllers are connected in series. One PI controller controls the outer voltage loop, and the other controls the inner current loop. The output is then converted to gate

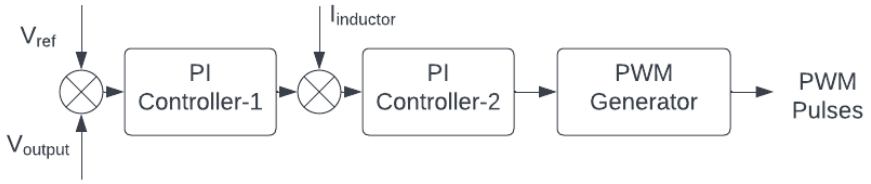

Figure 4.1. Block diagram of dual PI-tuned controller for SAB converter.

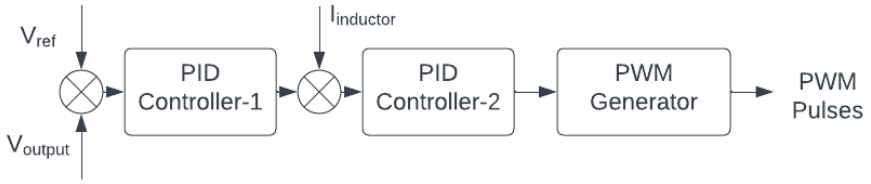

Figure 4.2. Block diagram of dual PID-tuned controller for SAB converter.

pulse for the SAB converter. The output voltage and the reference voltage are compared in the outer voltage loop. This output is then compared against reference inductor current at the input of HFT. Then the value is set and trigger signal is generated to obtain a fixed output voltage even when the input to the converter varies. The contribution of the controller to system stability decreases with increase in value of K_P or K_I. However, the steady state error decreases with increase in K_I.

4.3 PID Controller

The PID controller is a controller that can perform proportional, integral, and derivative control operations. The control signal exhibits proportionality with the error signal as well as the integral and derivative of the error signal. The general transfer function of a PID controller is given as

$$G(s) = K_P + \frac{K_I}{s} + K_D s \tag{4.3.1}$$

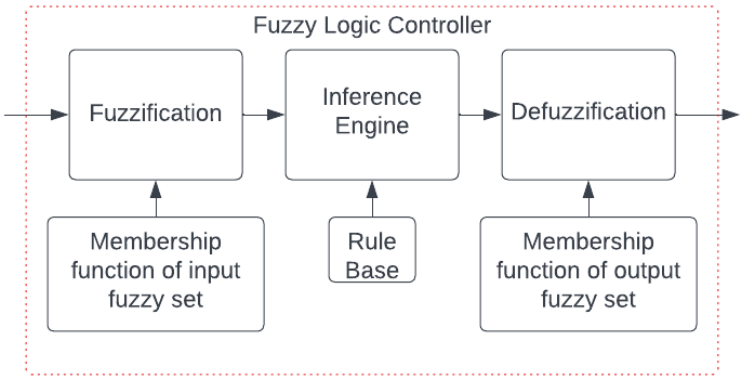

Figure 4.3. Schematic diagram of Fuzzy controller.

Two PID controllers are connected in series. Both the outer voltage loop and the inner current loop are under the control of separate PID controllers. The output is then converted to gate pulse for the SAB converter.Increasing the value of K_I decreases the oscillation in output voltage. However, the rise time and adjust time are longer. Increasing the value of K_D increases the adjust time and system becomes unstable, but the system reaction time becomes faster.

4.4 Fuzzy-PID Controller

The fundamental schematic diagram of a fuzzy logic controller is displayed in Fig. 4.3. A fuzzifier, an inference engine, and a defuzzifier make up this system. The fuzzifier creates fuzzy sets from the input's crisp value by a process known as fuzzification. Fuzzy outputs are produced by Inference Engine based on the fuzzy rules. The defuzzifier then produces the crisp output for various control purposes, known as defuzzification. Fuzzy inference system based on Mamdani is used for the proposed system as it is more intuitive and its rule bases are relatively easier to understand compared to Sugeno fuzzy inference system. The output of each rule in a mamdani system is a fuzzy set. This fuzzy set is obtained from the membership function of the outputs. The fuzziness in fuzzy logic is characterised

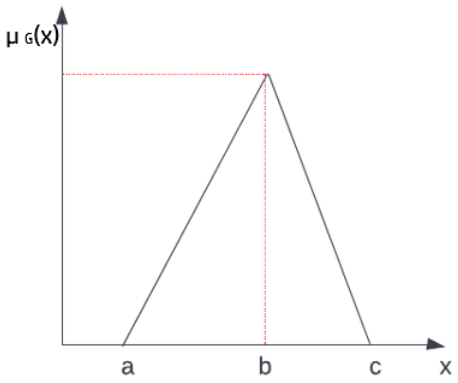

Figure 4.4. Representation of triangular membership function.

by membership functions. It is the graphical representation of a fuzzy set. They may have different shapes like sigmoid, triangular, gaussian, trapezoidal, etc. The membership function of a fuzzy set G is represented by $\mu_{\mathrm{G}}(\mathrm{x})$, where $\mu_{\mathrm{G}}(\mathrm{x})\ \epsilon\ [0,1]$. It represents the degree of membership of x in fuzzy set G.

Here triangular membership functions are selected as they are the most widely accepted. A triangular membership function has three basic parameters namely a, b and c, where for each x, the membership function $\mu_{\mathrm{G}}(\mathrm{x})$ is defined as follows:

$$\mu_{\mathrm{G}}(x) = \begin{cases} 0 & \text{if } \mathrm{x} \leq \mathrm{a} \\ \frac{x-a}{b-a} & \text{if } \mathrm{a} \leq \mathrm{x} \leq \mathrm{b} \\ \frac{c-x}{c-b} & \text{if } \mathrm{b} \leq \mathrm{x} \leq \mathrm{c} \\ 0 & \text{if } \mathrm{x} \geq \mathrm{c} \end{cases} \tag{4.4.1}$$

Fig.4.4 represents a triangular membership function with its parameters. The parameters are determined with the help of expert knowledge.

The inputs are error in voltage, E and change in error in voltage, CE. The outcomes are $\mathrm{K_P}$, $\mathrm{K_I}$ and $\mathrm{K_D}$. The fuzzy rules are as follows:

1. If (E is NL) and (CE is NL), then ($\mathrm{K_P}$ is PVL)($\mathrm{K_I}$ is PM)($\mathrm{K_D}$ is PVS)
2. If (E is NL) and (CE is NS), then ($\mathrm{K_P}$ is PVL)($\mathrm{K_I}$ is PM)($\mathrm{K_D}$ is PMS)
3. If (E is NL) and (CE is ZE), then ($\mathrm{K_P}$ is PVL)($\mathrm{K_I}$ is PM)($\mathrm{K_D}$ is PM)

4. If (E is NL) and (CE is PS), then (K_P is PVL)(K_I is PM)(K_D is PL)
5. If (E is NL) and (CE is PL), then (K_P is PVL)(K_I is PM)(K_D is PVL)
6. If (E is NS) and (CE is NL), then (K_P is PML)(K_I is PMS)(K_D is PMS)
7. If (E is NS) and (CE is NS), then (K_P is PML)(K_I is PMS)(K_D is PML)
8. If (E is NS) and (CE is ZE), then (K_P is PML)(K_I is PMS)(K_D is PL)
9. If (E is NS) and (CE is PS), then (K_P is PL)(K_I is PMS)(K_D is PVL)
10. If (E is NS) and (CE is PL), then (K_P is PVL)(K_I is PMS)(K_D is PVL)
11. If (E is ZE) and (CE is NL), then (K_P is PVS)(K_I is PS)(K_D is PM)
12. If (E is ZE) and (CE is NS), then (K_P is PVS)(K_I is PS)(K_D is PL)
13. If (E is ZE) and (CE is ZE), then (K_P is PS)(K_I is PVS)(K_D is PL)
14. If (E is ZE) and (CE is PS), then (K_P is PMS)(K_I is PS)(K_D is PVL)
15. If (E is ZE) and (CE is PL), then (K_P is PMS)(K_I is PS)(K_D is PVL)
16. If (E is PS) and (CE is NL), then (K_P is PML)(K_I is PMS)(K_D is PML)
17. If (E is PS) and (CE is NS), then (K_P is PML)(K_I is PMS)(K_D is PVL)
18. If (E is PS) and (CE is ZE), then (K_P is PML)(K_I is PMS)(K_D is PVL)
19. If (E is PS) and (CE is PS), then (K_P is PL)(K_I is PMS)(K_D is PVL)
20. If (E is PS) and (CE is PL), then (K_P is PVL)(K_I is PMS)(K_D is PVL)
21. If (E is PL) and (CE is NL), then (K_P is PVL)(K_I is PM)(K_D is PVL)
22. If (E is PL) and (CE is NS), then (K_P is PVL)(K_I is PM)(K_D is PVL)
23. If (E is PL) and (CE is ZE), then (K_P is PVL)(K_I is PM)(K_D is PVL)
24. If (E is PL) and (CE is PS), then (K_P is PVL)(K_I is PM)(K_D is PVL)
25. If (E is PL) and (CE is PL), then (K_P is PVL)(K_I is PM)(K_D is PVL)

Where, NL is Negative Large, NS is Negative Small, ZE is Zero, PS is Positive Small, PL is Positive Large, PVS is Positive Very Small, PMS is Positive Medium Small, PM is Positive Medium, PML is Positive Medium Large, PVL is Positive Very Large.

Fig.4.5 represents the membership functions of inputs, error and change in error. Fig.4.6 represents the membership functions of outputs, K_P, K_I and K_D.

Defuzzification is the process of mapping a fuzzy set to a crisp set. There exists a num-

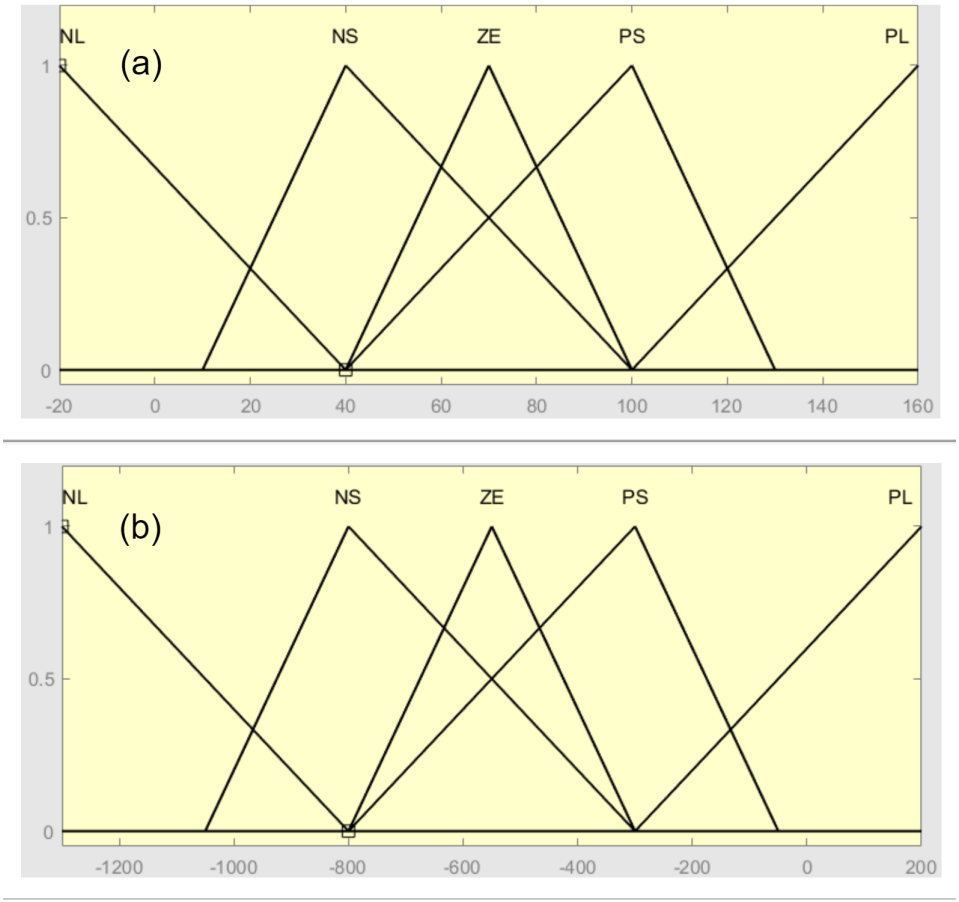

Figure 4.5. Membership funtions of inputs: (a) Error (b) Change in error

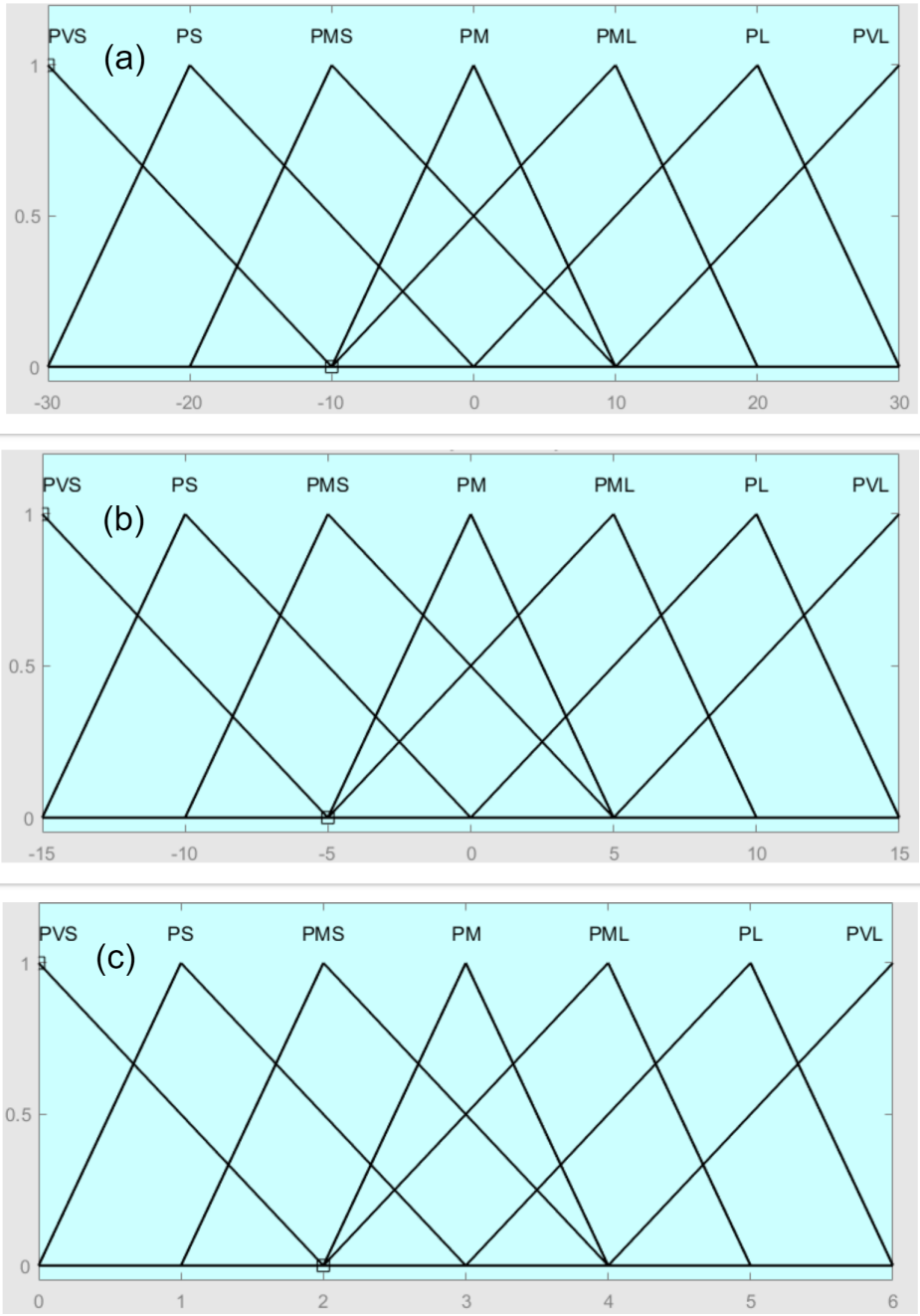

Figure 4.6. Membership funtions of outputs: (a) K_P (b) K_I (c) K_D

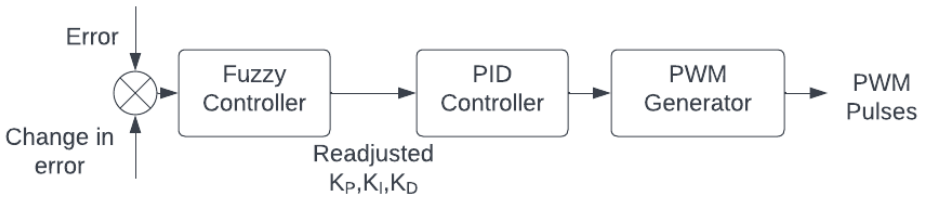

Figure 4.7. Block diagram of Fuzzy-PID controller for SAB converter.

ber of defuzzification techniques namely centroid, bisector, middle of maximum, smallest of maximum, largest of maximum, etc. This project uses the centroid approach. This method is also known as Centre Of Area method (COA).

Fig.4.7 shows the structure of Fuzzy-PID controller implemented for SAB converter. To calculate the error in voltage and change in error in voltage, the output voltage is compared to the reference voltage. These are then provided to the fuzzy controller as inputs. A rule base with two inputs is used to produce three outputs namely, readjusted K_P, K_I and K_D. These are then provided to the PID control and the associated gate pulses are fed to the switches of the SAB converter.

The generalized transfer function of Fuzzy-PID controller is given by

$$G(s) = K_{\mathrm{P}}(readjusted) + \frac{K_{\mathrm{I}}(readjusted)}{s}] + K_{\mathrm{D}}(readjusted)s \tag{4.4.2}$$

Where, K_P(readjusted), K_I(readjusted) and K_D(readjusted) are the readjusted proportional, integral and derivative gain respectively by the fuzzy logic controller.

Chapter 5

RESULTS AND DISCUSSION

5.1 Introduction

Using the SIMULINK in MATLAB software, the functionality of PI, PID, and Fuzzy-PID controllers for SAB converters is investigated and compared. The wind speed is at 20m/s from 0 to 0.5s and changes to 25m/s from 0.5s. The low voltage ac input from the WECS is then fed to the SST. The HVDC link capacitor couples the generator side and the grid side. The voltage observed across the HVDC link capacitor is maintained constant at 650V with the help of various controllers. Output voltage of 415V at 50Hz is integrated back into the utility grid. An HFT with 25kHz switching frequency and turns ratio 1:2 is selected. Fig.5.1 shows the simulation of proposed system in MATLAB/SIMULINK. Fig.5.2 shows the WECS with the pitch angle controller, wind turbine, two mass drive train and PMSG. The rated mechanical output power is taken as 8.5kW and the rated wind speed is taken as 153rad/s. Table 5.1 shows the simulation parameters and their values used for simulating the system.

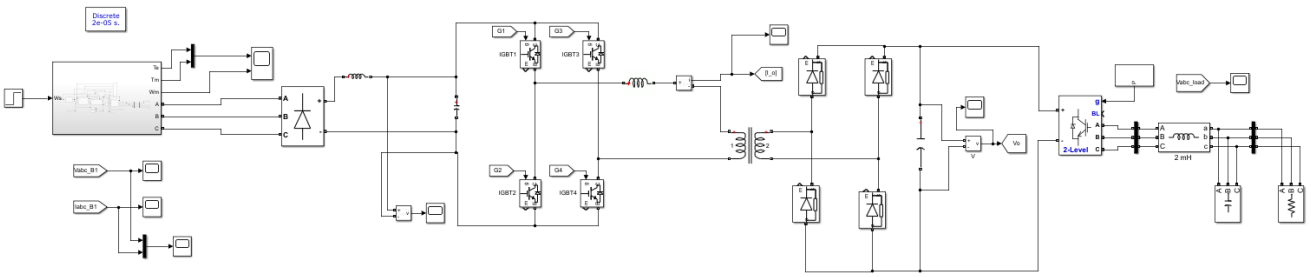

Figure 5.1. Block diagram of proposed system in MATLAB/SIMULINK.

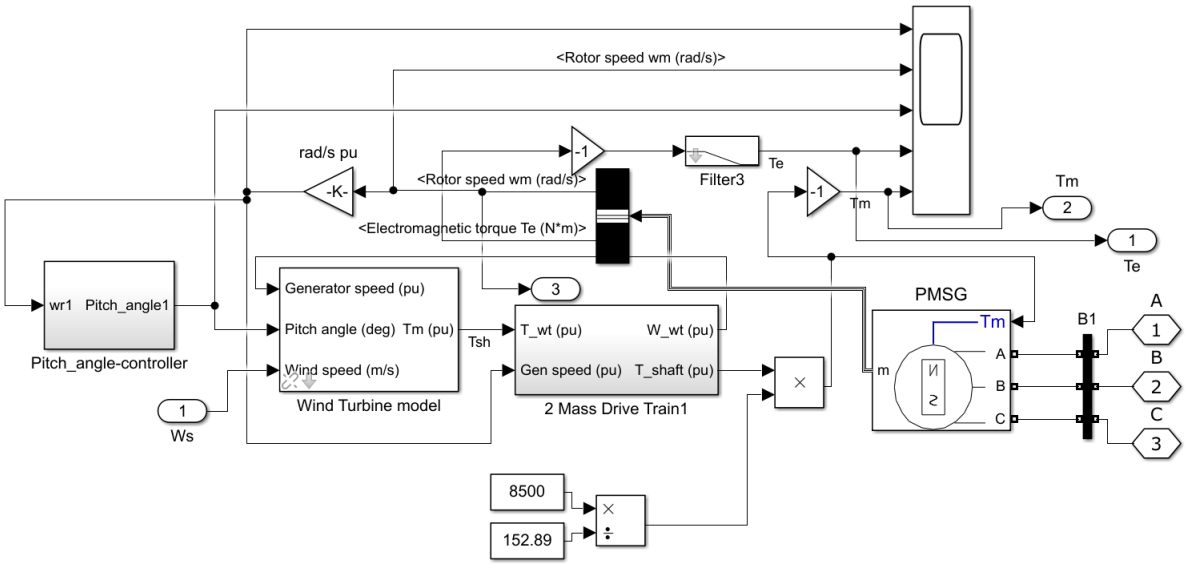

Figure 5.2. Block diagram of WECS in MATLAB/SIMULINK.

Table 5.1. Simulation Parameters

PARAMETER	VALUE
Rated power	1kVA
Range of input voltage to SST	200-400V
Switching frequency of DC-DC Converter	25kHz
HFT turns ratio	1:2
Transformer leakage inductance	5μH
Low voltage inductance	200μH
LVDC link capacitor	9000μF
HVDC link capacitor	88μF

5.2 Results- Closed loop system

Results were obtained for the system with PI, PID and Fuzzy-PID controller in SIMULINK under MATLAB software. Results were also obtained after the system was subjected to a disturbance for a period of time to analyse the performance following transients.

5.2.1 Closed loop simulation- PI Controller

Fig.5.3 shows the simulink model of system with dual PI-tuned controller in feedback path. K_P and K_I were tuned to optimise the system performance. Fig.5.4 shows the voltage across the HVDC link capacitor with dual PI-tuned controller. The rise time is 0.12s and settling time is 1s with a steady state value of 627V.

5.2.2 Closed loop simulation- PID Controller

Fig.5.5 shows the simulink model of system with dual PID-tuned controller in feedback path. K_P, K_I and K_D were tuned to optimise the system performance. Fig.5.6 shows the

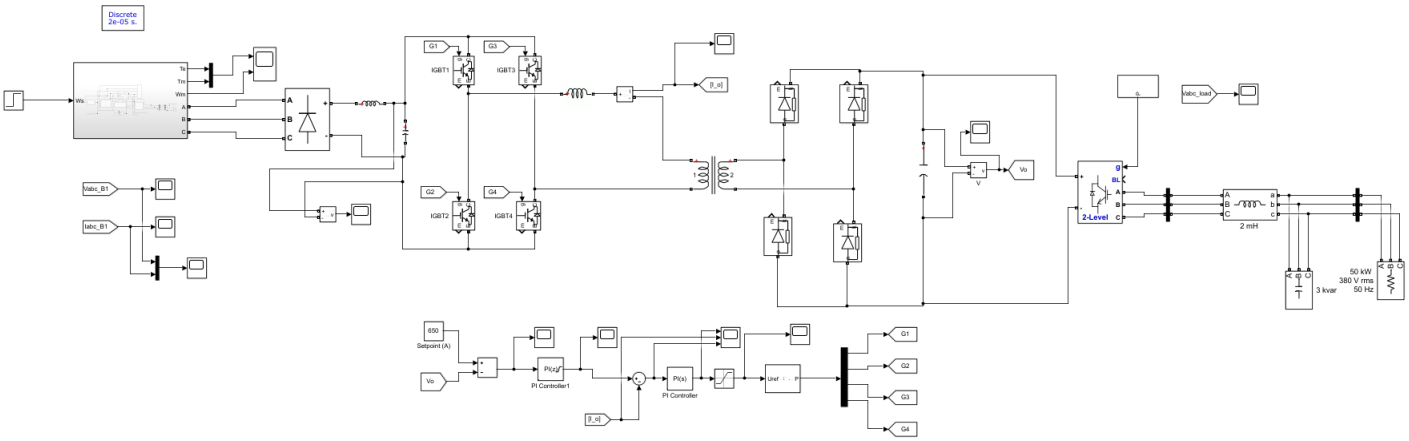

Figure 5.3. Simulation of system with dual PI-tuned controller.

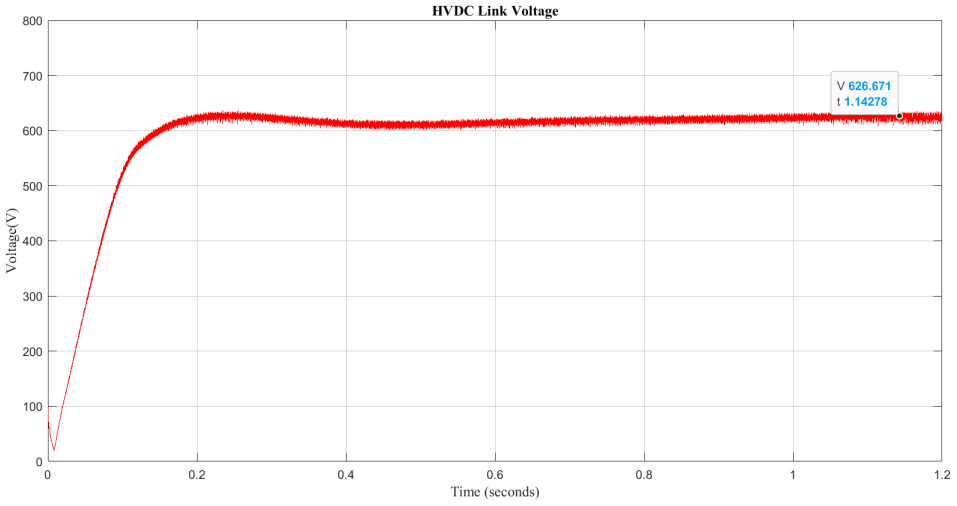

Figure 5.4. Voltage across HVDC link capacitor with dual PI-tuned controller.

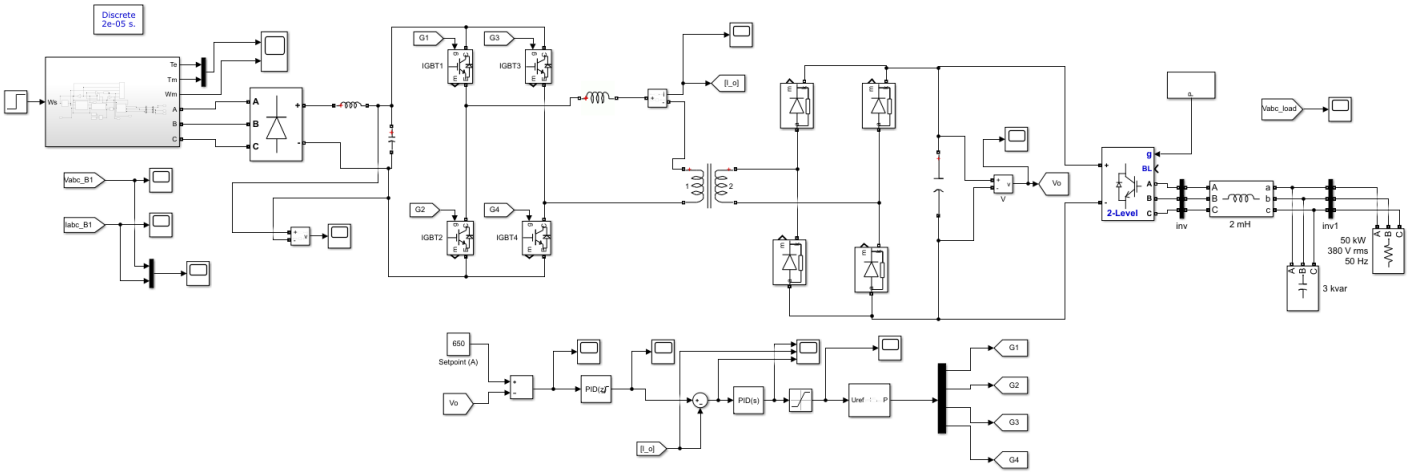

Figure 5.5. Simulation of system with dual PID-tuned controller.

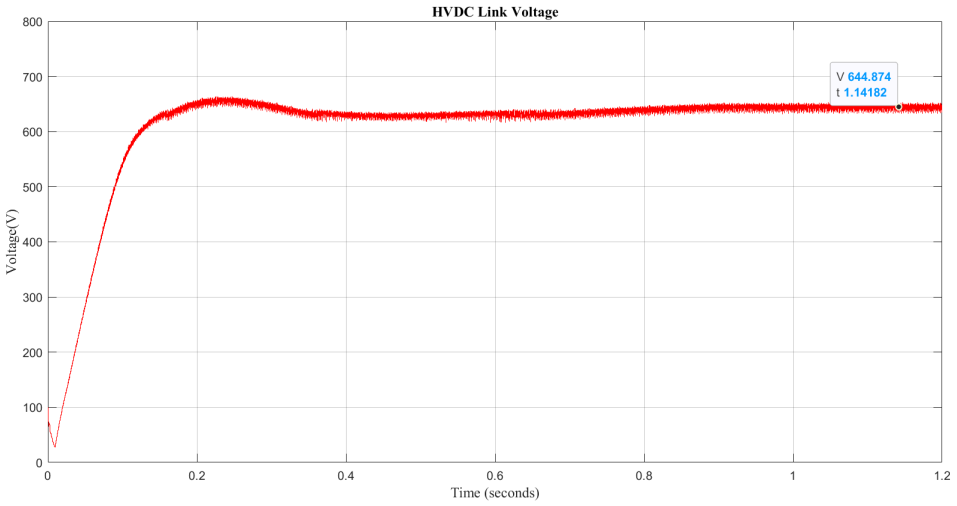

Figure 5.6. Voltage across HVDC link capacitor with dual PID-tuned controller.

voltage across the HVDC link capacitor with dual PID-tuned controller.The rise time is 0.114s and settling time is 0.9s with a steady state value of 645V.

5.2.3 Closed loop simulation- Fuzzy-PID Controller

Fig.5.7 shows the system simulation with Fuzzy-PID controller in feedback path. Fig.5.8 shows the simulink diagram of fuzzy-PID controller. The reference voltage(650V) and the HVDC link voltage are compared, to obtain the error in voltage and change in error in voltage. These are provided to the fuzzy logic controller as inputs to obtain the readjusted K_P, K_I and K_D. To create the gate pulses for the active bridge of the SAB converter, the PID controller's output is routed into a PWM generator. For the Fuzzy-PID controller only the voltage loop is considered, and the current loop is not taken into account.

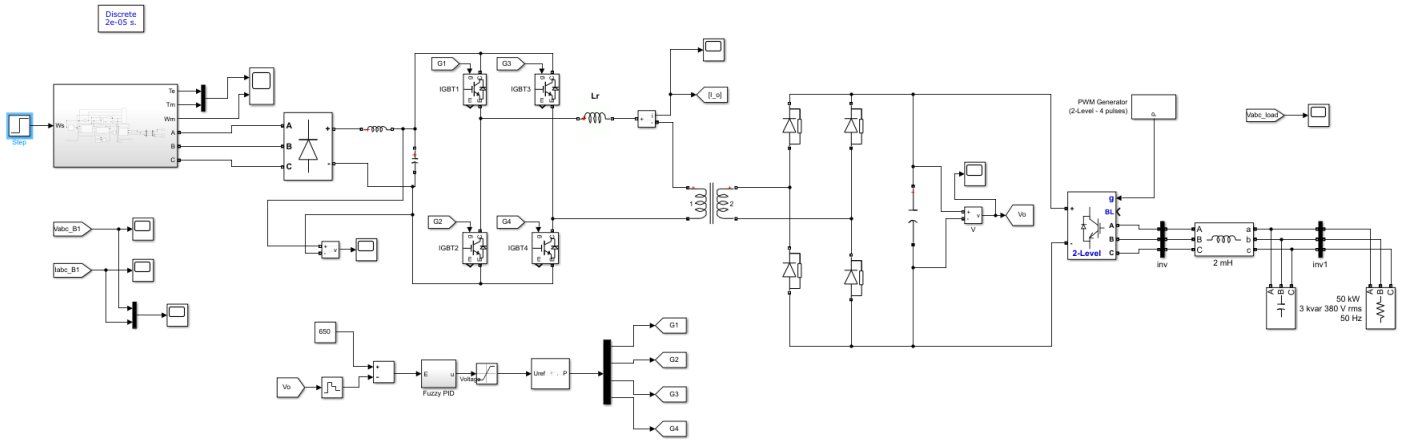

Figure 5.7. Simuation of system with Fuzzy-PID controller.

Fig.5.9 shows the voltage across the HVDC link capacitor with Fuzzy-PID controller. The rise time is 0.12s and settling time is 0.75s with a steady state value of 673V.

5.2.4 Analysis

PID shows better performance than PI controller. Fuzzy-PID controller offers better performance than both the other controllers. It has reduced ripples, reduced settling time,

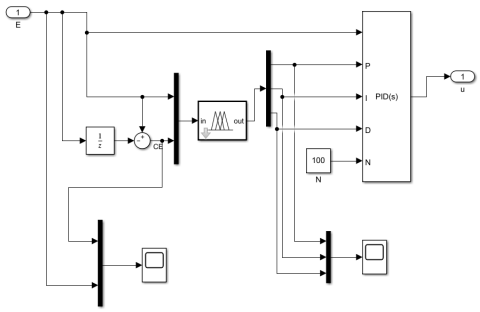

Figure 5.8. Simulink diagram of Fuzzy-PID controller.

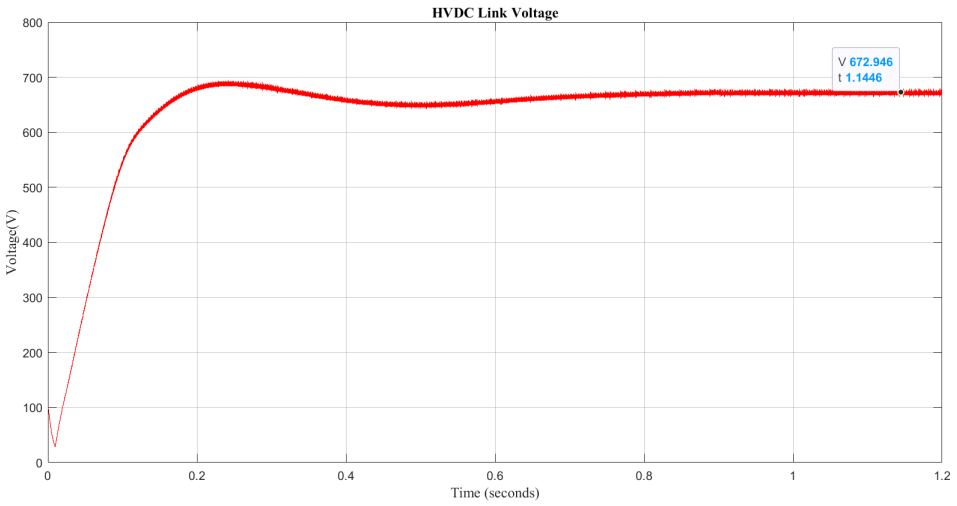

Figure 5.9. Voltage across HVDC link capacitor with Fuzzy-PID controller.

better rise time, etc. In Table 5.2, the effectiveness of the PI, PID, and Fuzzy-PID controllers for SAB converters is contrasted in terms of peak overshoot, rise time, settling time, and steady state voltage value.

Table 5.2. Comparison of controller performances

CONTROLLER	**Peak Overshoot(%)**	**Rise time(s)**	**Settling time(s)**	**Steady state value(V)**
PI	1.11	0.12	1	627
PID	2.3	0.114	0.9	645
Fuzzy-PID	2	0.12	0.75	673

5.3 Results- Disturbance analysis

Fig.5.10 shows the simulink diagram of system with a dual PI-tuned controller in feedback path with a disturbance introduced at 0.8s. Fig.5.11 shows voltage across the HVDC link capacitor with dual PI-tuned controller after a disturbance is introduced at 0.8s. Steady state is regained at 1s with a steady state value of 635V.

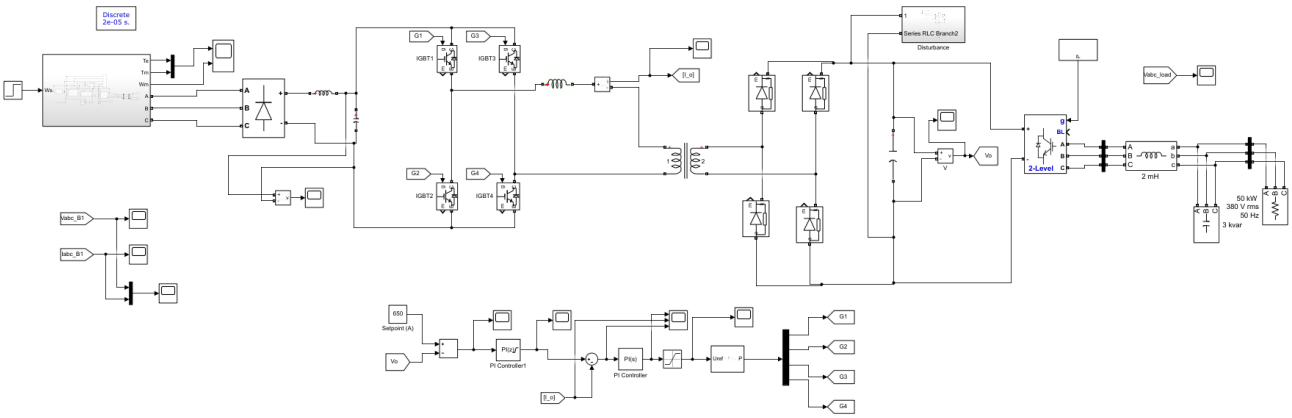

Figure 5.10. Simulation of system having dual PI-tuned controller with disturbance introduced at 0.8s.

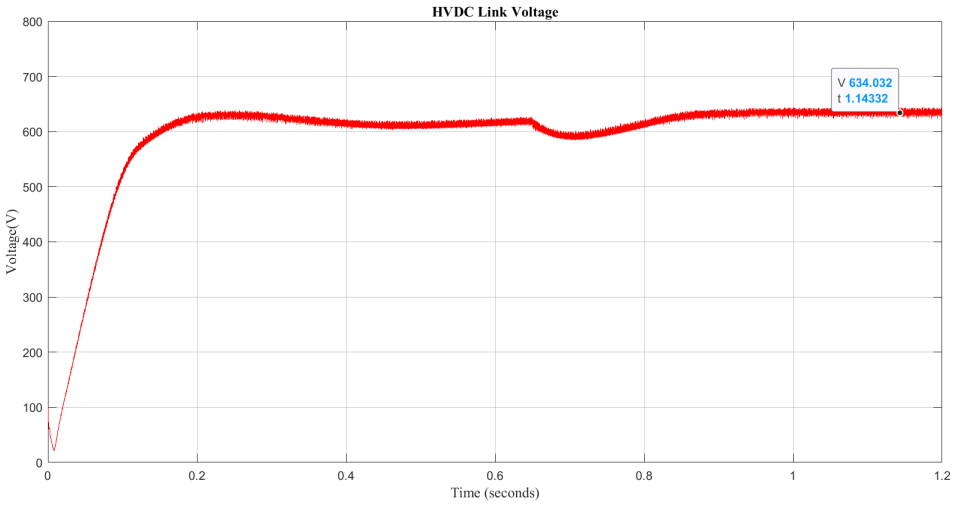

Figure 5.11. Voltage across HVDC link capacitor with dual PI-tuned controller with disturbance.

Fig.5.12 shows the simulink diagram of system with a dual PID-tuned controller in feedback path with a disturbance introduced at 0.8s. Fig.5.13 shows the voltage across the HVDC link capacitor with dual PID-tuned controller after a disturbance is introduced at 0.8s. Steady state is regained at 1s with a steady state value of 617V.

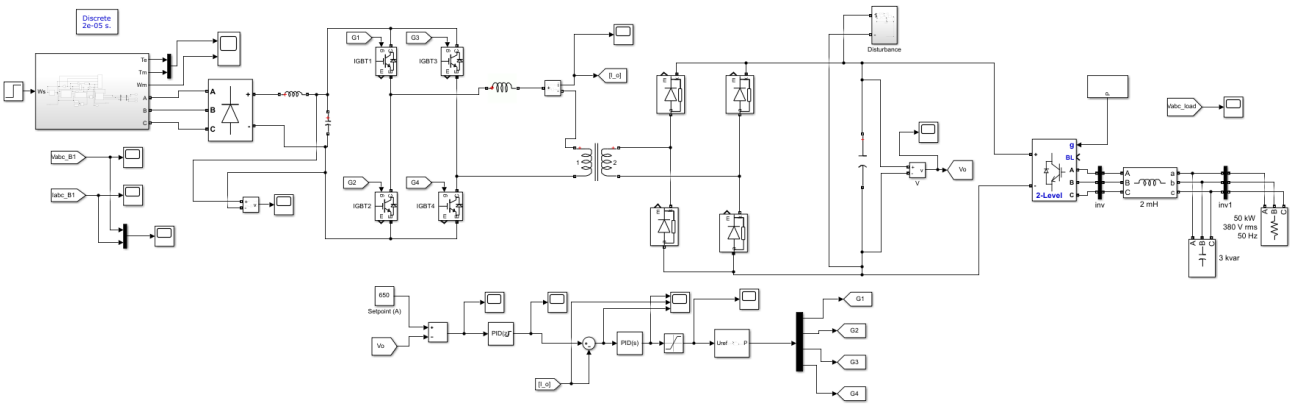

Figure 5.12. Simulation of system having dual PID-tuned controller with disturbance introduced at 0.8s.

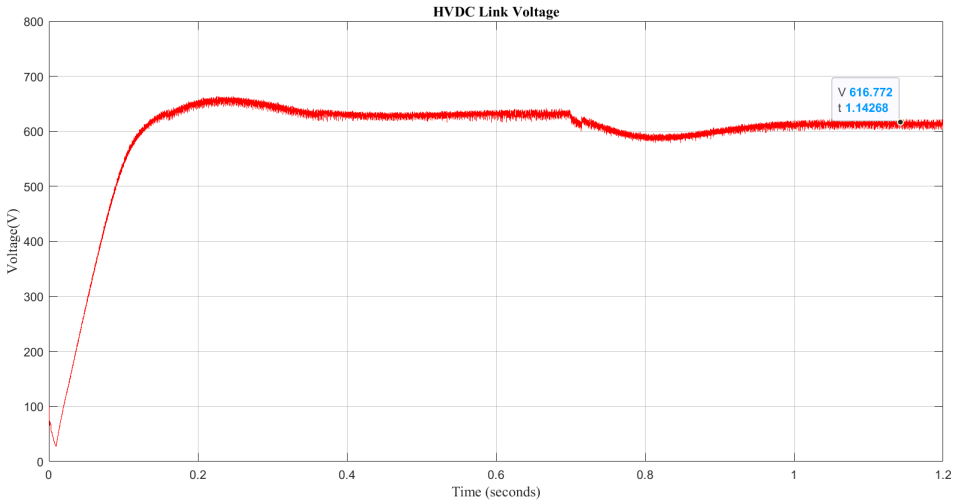

Figure 5.13. Voltage across HVDC link capacitor with dual PID-tuned controller with disturbance.

Fig.5.14 shows the simulink diagram of closed loop system with Fuzzy-PID controller with a disturbance introduced at 0.8s. Fig.5.15 illustrates the voltage across the HVDC link capacitor with Fuzzy-PID controller after a disturbance is introduced at 0.8s. Steady state is regained at 1.1s with a steady state value of 640V. Clearly, after introduction of disturbance, SAB converter with Fuzzy-PID controllers exhibits best performance in terms

of improved steady state voltage.

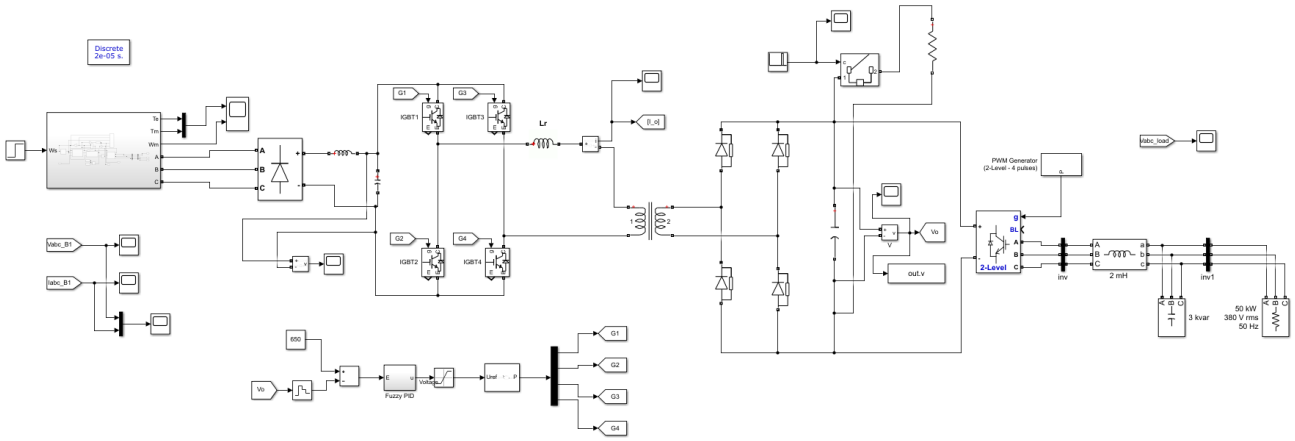

Figure 5.14. Simulation of system having Fuzzy-PID controller with disturbance introduced at 0.8s.

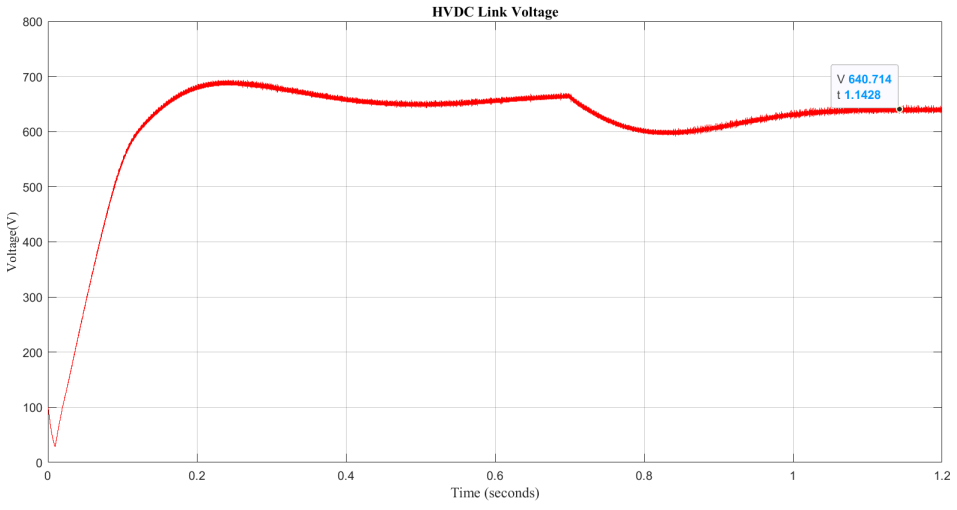

Figure 5.15. Voltage across HVDC link capacitor with Fuzzy-PID controller with disturbance.

Chapter 6

CONCLUSION

The PMSG based WECS and the SST were simulated in SIMULINK under MATLAB software. The performance of SAB based SST with PI, PID and Fuzzy-PID controllers is studied and compared. The WECS is modelled and implemented to produce low voltage wind energy input to the SST. Even when the wind speed is varied from 20m/s to 25m/s, the voltage across the HVDC link capacitor of the SST is regulated at almost 650V. Performance-wise, fuzzy-PID controllers outperform both PI and PID with reduced ripples, reduced settling time, better rise time and a peak overshoot of 2%. Even after the introduction of disturbance, best result is offered by the Fuzzy-PID controller with better steady state performance. It attains a steady state value of 640V at 1.1s.

PUBLICATIONS

[1] Keerthi Gopal D, Shanavas T.N, Naufal.N(2022), "Solid State Transformers for Smart grid Control and Applications- A Review," Communicated to International conference on Futuristic Technologies in Control Systems Renewable Energy (ICFCR 2022).

REFERENCES

[1] **E.J. Coster, J.M.A Myrzik, B. Kruimer, and W. L. Kling**(2011), "Integration Issues of Distributed Generation in Distribution Grids," *Proceedings of the IEEE*, vol. 99, no. 1.

[2] **Imran Syed, and Vinod Khadkikar**(2017), "Replacing the Grid Interface Transformer in Wind Energy Conversion System With Solid-State Transformer," *IEEE Transactions on Power Systems*, vol. 32, no. 3.

[3] **J. Chen, R. Zhu, T. Oldonnell, and M. Liserr**(2018), "Smart transformer and low frequency transformer comparison on power delivery characteristics in the power system," *in Proc. 110th AEIT Int. Annu. Conf. AEIT.*

[4] **X. Liang**(2017), "Emerging power quality challenges due to integration of renewable energy sources," *IEEE Transactions on Industrial Applications*, vol. 53.

[5] **A. Milczarek and M. Malinowski**(2019), "Comparison of classical and smart transformers impact on MV distribution grid," *IEEE Transactions on Power Delivery*, vol. 30.

[6] **Subhadeep Paladhi and Ashok S**(2015), "Solid State Transformer Application in Wind Based DG System," *in IEEE International Conference on Signal Processing, Informatics, Communication and Energy Systems (SPICES).*

[7] **Giovanni De Carne, Giampaolo Buticchi, Zhixiang Zou and Marco Liserre**(2018), "Reverse Power Flow Control in a ST-Fed Distribution Grid," *IEEE Transactions on Smart Grid.*, vol. 9.

[8] **Stefano Giacomuzzi, Marius Langwasser, Giovanni De Carne, Giuseppe Buja, and Marco Liserre**(2020), "Smart Transformer-based Medium Voltage Grid Support by Means of Active Power Control," *CES Transactions on Electrical Machines and Syst.*, vol. 4, no. 4.

[9] **Rongwu Zhu, Giovanni De Carne, Fujin Deng, and Marco Liserre**(2017), "Integration of Large Photovoltaic and Wind System by Means of Smart Transformer," *IEEE Transactions on Industrial Electronics*, vol. 64, no. 11.

[10] **J. Subhadeep Paladhi and Ashok S**(2015), "Power Quality Improvements in Wind Based DG Systems using Solid State Transformer," *International Journal of Scientific Engineering Research*, vol. 6, no. 4.

[11] **Mahammad A. Hannan, Pin Jern Ker, Molla S. Hossain Lipu, Zhen Hang Choi, M. Safwan Abd. Rahman, Kashem M. Muttaqi and Frede Blaabjerg**(2020), "State of the Art of Solid-State Transformers: Advanced Topologies, Implementation Issues, Recent Progress and Improvements," *IEEE Access*, vol. 8.

[12] **S. Falcones, X. Mao, and R. Ayyanar**(2010), "Topology comparison for solid state transformer implementation," *in Proc. IEEE PES Gen. Meeting.*

[13] **Subhadeep Paladhi and Ashok S**(2015), "Solid State Transformer Application in Wind Based DG System," *Signal Processing, Informatics, Communication and Energy Systems (SPICES), in 2015 IEEE International Conference.*

[14] **J. E. Huber, and J. W. Kolar**(2014), "Volume/weight/cost comparison of a 1MVA 10 kV/400 V solid-state against a conventional low-frequency distribution transformer," *in Proc. IEEE Energy Convers. Congr. Expo.. (ECCE).*

[15] **Hemant Ahuja, G. Bhuvaneswari and R. Balasubramanian**(2011), "Performance Comparison of DFIG AND PMSG based WECS," *IET Conference on Renewable Power Generation.*

[16] **L. F. Costa, G. De Carne, G. Buticchi, and M. Liserre**(2017), "The smart transformer: A solid-state transformer tailored to provide ancillary services to the distribution grid," *IEEE Power Electron. Mag.*, vol. 4, no. 2.

[17] **Neetu Singh and Dr Bhupal Singh**(2016), "Simulink Based Modeling, Design and Performance Evaluation of PMSG Based Wind Energy Conversion System," *Journal of Multi Disciplinary Engineering Technologies.*

[18] **Rupendra Kumar Pachauri and Yogesh K. Chauhan**(2014), "Mechanical Control Methods in Wind Turbine Operations for Power Generation," *Journal of Automation and Control Engineering*, vol. 2, no. 3.

[19] **Bhende, C.N., Misra, S. and Malla, S.G.**(2011), "Permanent magnet synchronous generator based standalone wind energy supply system," *IEEE Trans. Sustainable Energy*, vol. 2, no. 4.

[20] **Christian Fontana, Mattia Forato, Kundan Kumar, Maria T. Outeiro, Manuele Bertoluzzo, and Giuseppe Buja**(2015), "Soft-switching capabilities of SAB vs. DAB converters," *IECON 2015 - 41st Annual Conference of the IEEE Industrial Electronics Society.*

[21] **Kiam Heong Ang, Gregory Chong, and Yun Li**(2015), "PID Control System Analysis, Design, and Technology," *IEEE Transactions on Control Systems Technology*, vol. 13, no. 4.

[22] **Lalitesh Kumar, Prawendra Kumar, and Subhojit Ghosh**(2014), "Design of PI Controller:A Multiobjective Optimization Approach," *International Conference on Advances in Computing,Communications and Informatics (ICACCI) .*

[23] **Sneha Mariam Sam and T.S. Angel**(2017), "Performance Optimization of PID Controllers using Fuzzy Logic," *IEEE International Conference on Smart Technologies and Management for Computing, Communication, Controls, Energy and Materials (ICSTM).*